# Glassy cholesteric structure: thickness variation induced by electron radiation in transmission electron microscopy investigated by atomic force microscopy

A. Boudet, Michel Mitov, C. Bourgerette, T. Ondarçuhu, R. Coratger

Accepted version published in: *Ultramicroscopy*, **88**, 219-229 (2001).

# Glassy cholesteric structure: thickness variation induced by electron radiation in transmission electron microscopy investigated by atomic force microscopy

A. Boudet, M. Mitov*, C. Bourgerette, T. Ondarçuhu, R. Coratger

CEMES-CNRS, BP 4347, F-31055 Toulouse Cedex 4, France

During the observation of glassy cholesteric liquid crystals in transmission electron microscopy (TEM), a new contrast is created or enhanced by electron radiation which has a direct relationship with the periodic microstructure of the specimen. In this paper, we investigate the variations of the sample thickness and mass density as possible causes of this irradiation contrast. By means of observations in atomic force microscopy (AFM) coupled to TEM, we compared the surface corrugations of non-irradiated and irradiated specimens. It is shown that the final contrast is the result of several processes, including fracture during ultramicrotomy and mass loss during irradiation. Mass loss acts as an etching, and hence results in a decrease of the sample thickness. The etching depends on the initial molecular orientation, thus evidencing the latent structure. An electron channelling mechanism is suggested to explain this behaviour.

Keywords: Radiation effects; Transmission electron microscopy; Atomic force microscopy; Electron channeling

*Email address: mitov@cemes.fr

*Article history*: Received 11 September 2000; received in revised form 9 March 2001.

https://doi.org/10.1016/S0304-3991(01)00087-0

Accepted version published in: *Ultramicroscopy*, **88**, 219-229 (2001).

## 1. Introduction

The characteristics and properties of polymers and other organic substances greatly depend on their microstructure at the level of the nanometer to micrometer scale, so that their observation in transmission electron microscopy (TEM) is of great interest [1]. This is particularly true for polymers developed thanks to new ways of synthesis and processing allowing their molecular architecture to be engineered. For example in liquid crystals, the microstructure is partly controlled by the design of the molecule and by self-organisation of the anisotropic molecules [2]. In previous studies [3,4], we have given an example of an assessment of such a direct relation between the microstructure and the optical properties of liquid crystals. Well-oriented cholesteric specimens with a progressive pitch showed selective light reflections in a controlled range of the visible light wavelengths. The direct visualisation of their structures by TEM revealed that the cholesteric periodicities are well oriented and progressively distributed in a range of values exactly fitting the reflected light wavelengths. However, the observations in TEM of liquid crystals, liquid crystal polymers, or other polymers and, more generally, all organic substances are limited by the low contrast exhibited by these materials and by the radiation damage undergone by the specimens inside the microscope. It has long been established that a loss of mass occurs [5,6], and that crystalline specimens are damaged and changed into an amorphous material [5,7–10]. The remaining contrast is due only to variations of mass density or of thickness or both. Any diffraction contrast is very transient, so special methods of contrast have to be used, like introducing stains to obtain different mass densities, or creating an artificial variation of thickness by selective etching [1]. However, in some rare cases, a new contrast is created by irradiation, directly related to the microstructure of the specimen. Enhancement of contrast due to radiation has already been noticed in spherulites of polyethylene [11,12], of polyamide and polypropylene [8]. For example, in polyethylene spherulites, radiation damage reveals concentric rings, which are related to the initial periodic twisting of the crystalline lamellas [11]. Enhancement of contrast

by irradiation has also been addressed in cholesteric liquid crystals [13]. In our own studies [4,14], we showed images of a glassy cholesteric liquid crystal taken in TEM. We studied the relation between this contrast due to irradiation and diffraction contrast before damaging [14]. The low contrast of alternate bright and dark lines was interpreted as the helical variation of the molecular orientation in the cholesteric structure. Though this type of contrast is currently seen in polarised light microscopy as a result of the birefringence of the liquid crystal, in TEM the contrast mechanism was unclear and we demonstrated its diffraction origin. From dark field images and oriented diffraction patterns, it was established that the mesogenic molecules in the dark lines are parallel to the lines and in the plane of the substrate, whereas they are perpendicular to the substrate in the bright lines (Fig. 1).

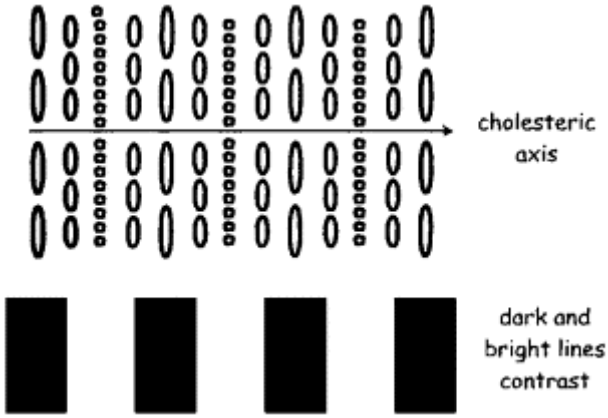


Fig. 1. A sketch showing the correspondence between the contrast in TEM and the molecular orientation.

During the observation, as radiation proceeds, the lines first disappear, then a new contrast rises up, the lines reappear and become more and more visible. Nevertheless, the diffraction pattern remains typically characteristic of an amorphous substance, so that the contrast must be due to a periodic variation of density or thickness of the sample. What is the cause of this irradiation contrast? Is it due to a variation of thickness or of mass density? And through what molecular mechanisms can it be so closely related to the initial cholesteric order, which is now

destroyed? In this paper, we give a partial answer to these questions by means of observations in atomic force microscopy (AFM) coupled to TEM. AFM is able to measure and display the relief of the surface. Other authors have conducted observations in AFM of non-irradiated or irradiated cholesteric liquid crystals [13,15–18] and all of them have seen periodic undulations of the surface. Some have carried out their observations on free surfaces where these undulations can develop freely but without correlation with TEM [16–18]. Others have been made on slices cut by ultramicrotomy and related to TEM observations [13,15]. The undulations appear to be produced by cutting before irradiation. Bunning et al. [13] claimed that contrast is due to a variation of the sample mass density projected onto the 2D observation plane, and not to a thickness variation. Our studies reported here lead to the interpretation that several processes are at work, but that we are mainly dealing with variation of thickness caused by differential etching.

## 2. Materials

The specimens studied in this paper are the same as in [4]. The liquid crystals themselves are the same glassy cholesteric liquid crystals as in [3,4,14,19,20], and the same contrast of parallel lines is observed after radiation damage. The original films were made of a cholesteric oligomer, the molecule of which is a cyclic siloxane with two types of side-chains attached by a spacer to the main chain (Fig. 2) [21]. One is chiral and the other not, so that the cholesteric pitch is tuned by the choice of the chiral side-chain percentage. Two different films were studied, one reflecting in the blue range named SB, with 50% chiral side-chains, one reflecting in the red range, named SR, with 31% chiral side-chains. The glass transition occurs between 40°C and 55°C and the cholesteric–isotropic transition at 180–200°C. The cholesteric pitch for SB is 290 nm, and for SR, 480 nm. Several specimens are made of a double layer SB–SR which is changed into a single layer by an annealing process during a determined length of time. Other characteristics can be found in [3,4,14,20].

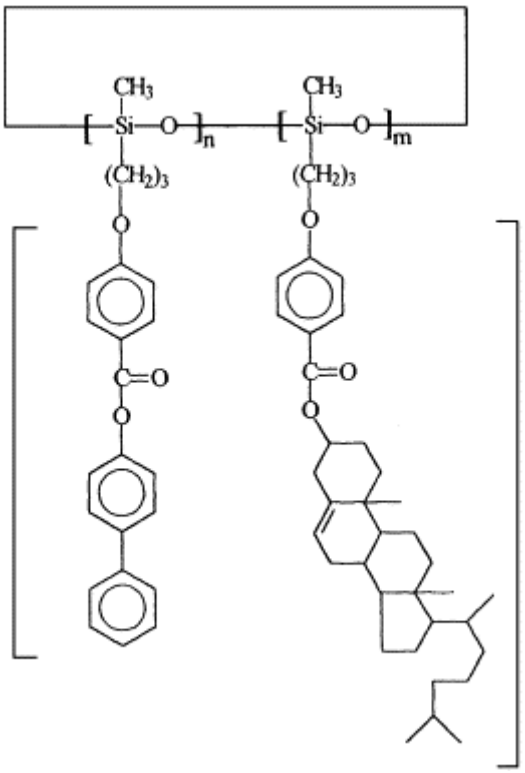

Fig. 2. A sketch of the molecule of the cholesteric liquid crystal.
The degree of polymerization $n + m = 5–7$.

### 3. Characterisation methods

To prepare the specimens for TEM, 40 μm thick films were made by melting between two glass slides in the following process: 12 h at 160°C, and then quenched to room temperature in a glassy state. Ultrathin sections were then prepared from the bulk material with an ultramicrotome (Reichert Ultracut S) using a diamond knife. Some specimens were ‘‘sandwiches’’ made for the study in [4,22]. SB and SR films were made separately on glass slides, then stacked together and heated on a heating stage at 85°C during a determined time. At this temperature, the films are both in their cholesteric phase and rather fluid, so that they are able to move and diffuse. The times of annealing varied between 5 min and 83 h. TEM observations were carried out with Philips CM12 and CM20 microscopes operating at 120 and

200 kV, respectively. The intensity of the electron beam on the specimen was set at 1.8 e/nm$^2$ s at low magnifications (x1200) and was strongly increased (up to 5000 e/nm$^2$ s) for irradiation purposes in some observations as reported below. AFM was performed either in contact mode on a Nanoscope II microscope (Digital Instruments) or in tapping mode on a Dimension 3000 (Digital Instruments).

## 4. Surface variation: observation of irradiated specimens in atomic force microscopy

Transversal sections of specimens were obtained by ultramicrotomy, observed and irradiated in TEM, and the specific contrast was recorded. Then, to understand this contrast, the surfaces of these specimens were imaged by AFM. Fig. 3 is a TEM micrograph showing a transverse section of a double SB–SR layer annealed for 83 h.

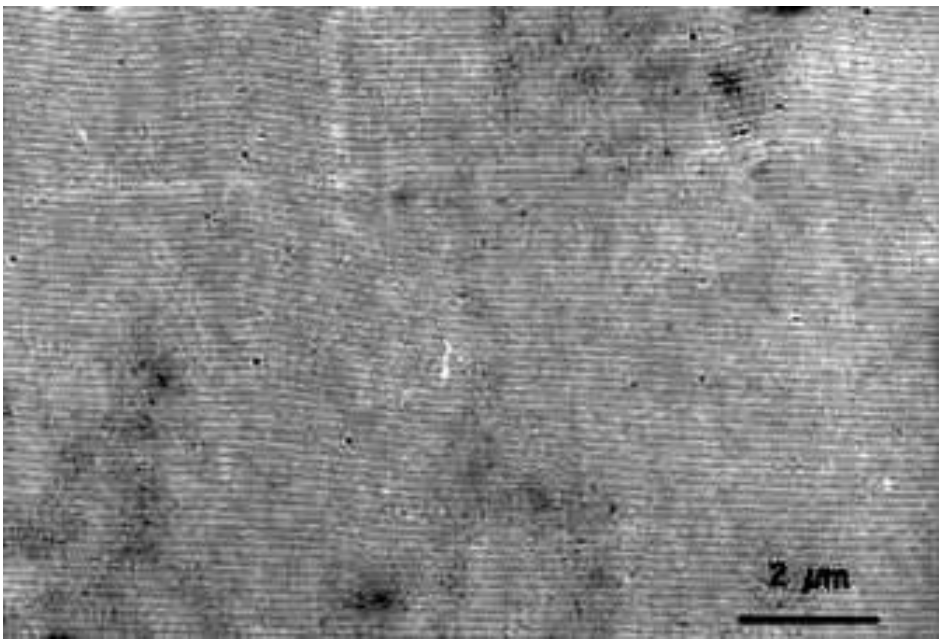


Fig. 3. Cross-section of a cholesteric sample showing the light and dark line alternation. Sample annealed during 83 h. TEM (bright field).

For reasons discussed in [3], this treatment allows the two materials to diffuse one into the other. On this irradiated specimen, the cholesteric periodicity is well seen, the value of which

(160 nm) is midway between the values of the SB and SR half-pitches. The corresponding diffraction pattern is typical of an amorphous substance, so that the contrast only arises from density or thickness. More precisely, a third type of contrast is involved here, phase contrast due to possible defocus, but this is perfectly controlled and disappears at exact focusing, where the periodic lines remain visible. Defocusing is a simple way to enhance the visibility of the lines which are basically due to density and thickness. We have already published other such pictures in [4].

A typical surface of the same specimen is shown in Fig. 4 by AFM. Outstanding periodic corrugations with alternating valleys and ridges with a regular height can be seen. The value of the periodicity is 166 nm, in close agreement with the values measured in TEM (see also [4]). On this view, the peaks are 4–5nm high, and on other parts the height can vary from 3 to 9 nm. This is a strong indication that the contrast corresponds to variations of thickness, if the lower surface has no particular relief. However, it cannot be excluded that this lower surface have corrugations strictly parallel to the upper surface, as proposed in [13], but this would be a very unlikely situation, as discussed in the next section. Now, why should such corrugations occur on a surface cut flatly and evenly by the microtome? Two mechanisms are likely to be involved. The corrugations may arise during cutting, or be provoked by irradiation, or both. In order to discriminate between the two phenomena, we studied non irradiated surfaces after cutting.

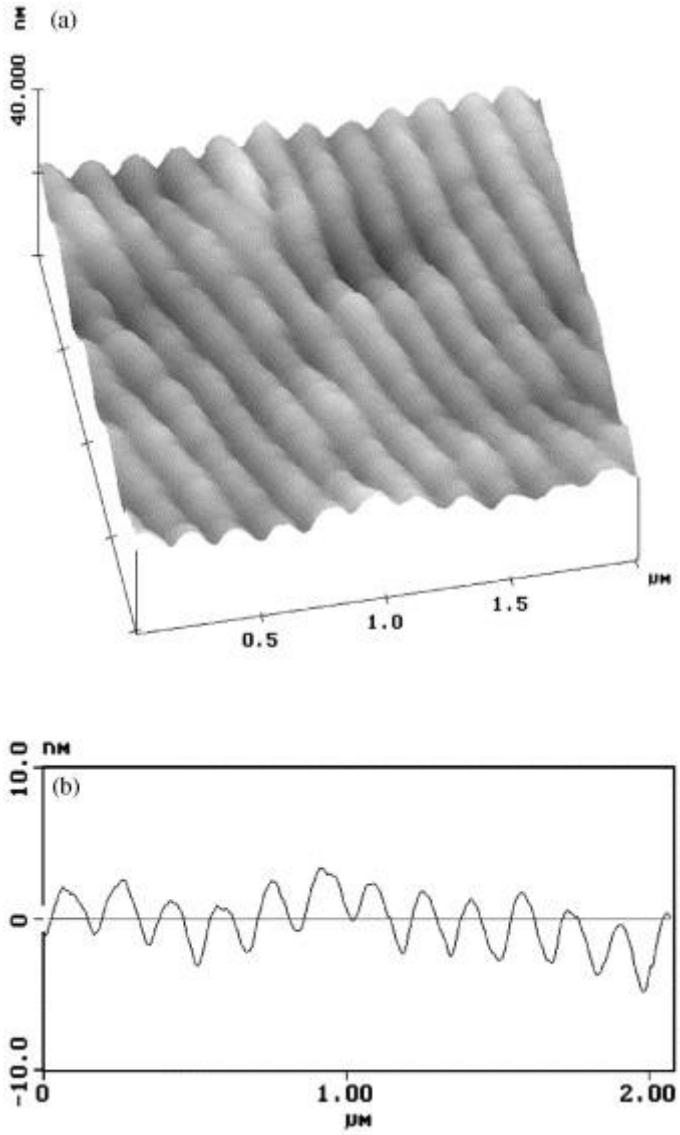


Fig. 4. Same sample as in Fig. 3, irradiated in TEM, viewed in AFM. (a) 3D image; (b) profile along a line perpendicular to the periodicities.

## 5. Cutting effects: observation of non-irradiated specimens in atomic force microscopy

Transversal sections of several specimens were made by ultramicrotomy and prepared on grids for examination in TEM, and their upper surfaces were observed in AFM before being irradiated in TEM. One of these images is shown in Fig. 5.

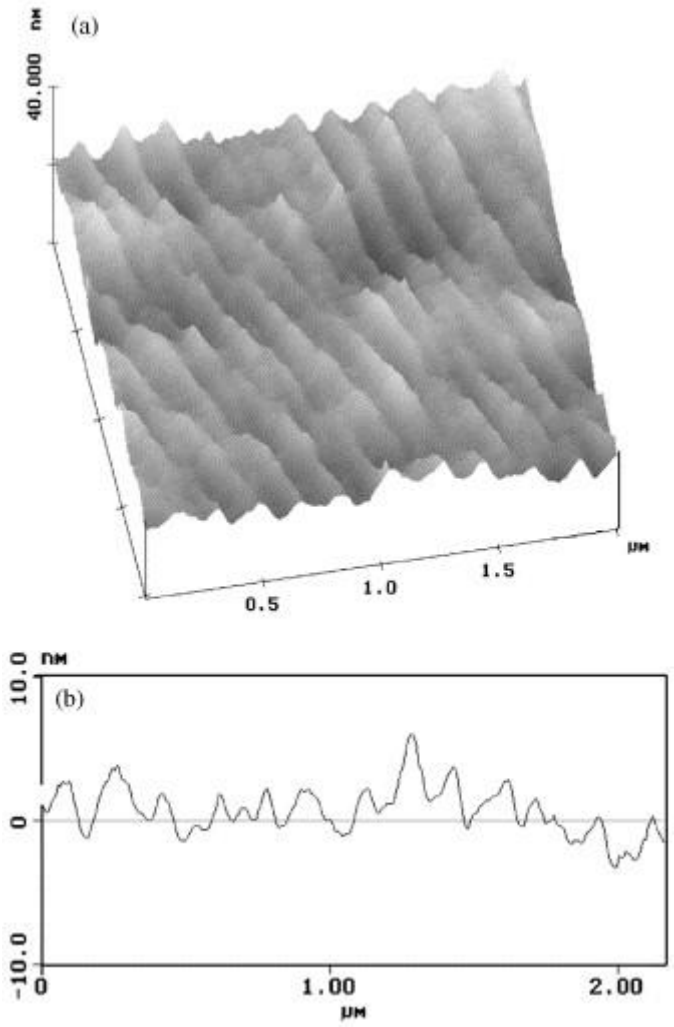


Fig. 5. Same sample as in Fig. 3 viewed in AFM before irradiation. (a) 3D image; (b) profile along a line perpendicular to the periodicities.

The surface is not even, but bumpy and irregular. The cholesteric periodicities show up clearly, but they are not so pronounced as in irradiated specimens. On larger views, tracks due to the ultramicrotome knife can be seen. In the corrugation profile of this view, the peak heights are uneven, about 2–6 nm, values close to those measured in the irradiated specimens. In some other specimens, the periodicities in the fracture surface are rare and visible only at some areas. Most of the surface is covered by random corrugations (Fig. 6).

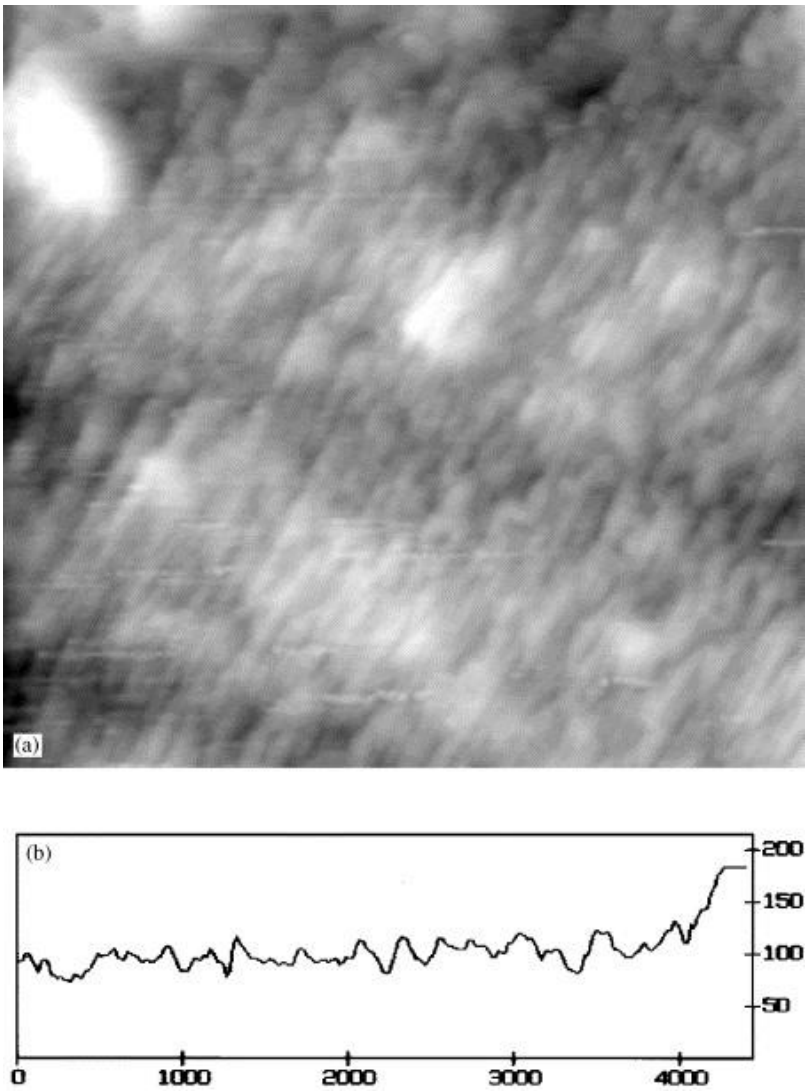


Fig. 6. Non-irradiated sample viewed in AFM (a) topological image; (b) profile.

From these observations, it is clear that corrugations corresponding to the cholesteric periodicities are due to cutting and that they result from the interaction between the knife and the specimen structure. Instead of going evenly, the knife creates a fracture surface that is influenced by the internal cholesteric periodicity, or, in other words, by the disposition of the molecule orientations. Corrugations due to microtomy have already been noticed on biological cholesteric materials studied in optical microscopy by Giraud-Guill!e [23] and Bouligand [24]. In a very fine analysis, Bouligand supported the hypothesis that the knife alternatively passes

between molecules or cuts them, making steps on both sides of the section, which can be shifted with respect to one another and consequently producing a periodically varying thickness (Fig. 7).

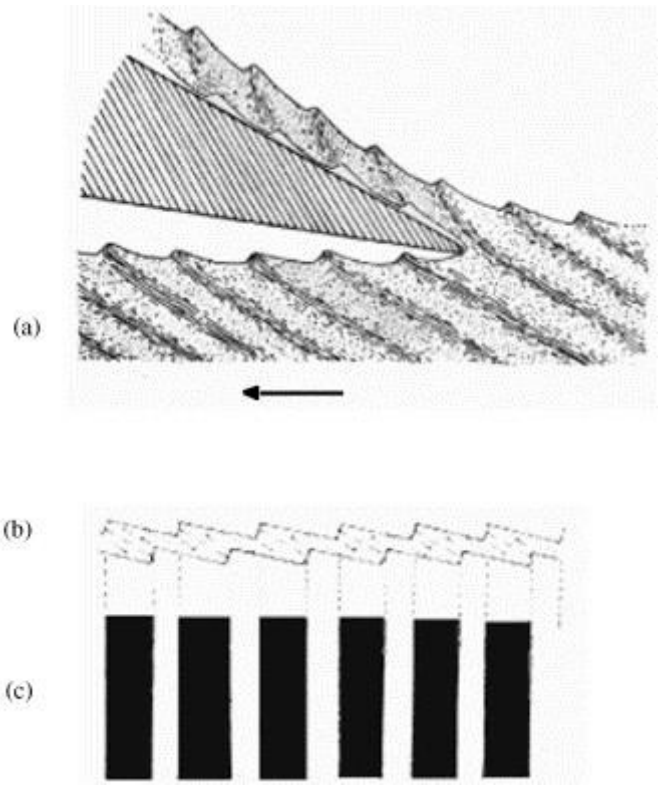


Fig. 7. A sketch of the occurrence of corrugations due to cutting (b); in relationship with molecular orientation (a); in relationship with contrast in TEM (c). From [23].

Our own observations are in agreement with these deductions, and it is only for a particular optical axis that a constant thickness would be crossed by the electron beam. As noticed by Huang et al. [15], the mechanical deformation due to the knife could vary if the knife passed in different orientations with respect to the molecules, but they found no such effect. To check whether it has an influence on our specimens, we carried out observations on cross-sections cut along the periodicities or perpendicular to them (Fig. 8).

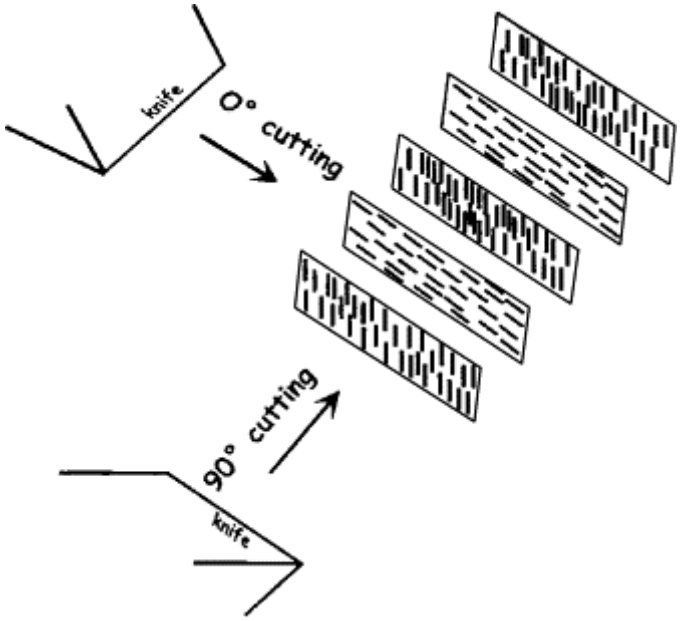


Fig. 8. A sketch of the relative orientation of the ultramicrotome knife and the molecules in a cross-section of a cholesteric structure.

According to the model of Fig. 1, the knife alternatively cuts the molecules stemming from the surface perpendicularly and passes along the ‘‘horizontal’’ molecules for a zero cutting angle. Remaining in the cross-section, a variation of the cutting angle to 90° does not change the orientation of the knife with respect to the vertical molecules whilst the horizontal molecules are scanned perpendicularly. This could give rise to some effects. This phenomenon is already known in side chain liquid crystal polymers. We demonstrated by electronic diffraction that the molecules lying in the cross-section were tilted by the knife, and we found that the resulting tilt angle after relaxation was proportional to their orientation with respect to the sectioning direction [25]. Now, observations have been conducted for different cutting angles (0°, 45° and 90° to the line orientation). No evidence of differences was noticeable by AFM. This indicates that the differences of angles of molecules lying in the cross-section do not induce sufficiently strong effects to be noticed, compared to the difference that exists between these horizontal molecules and the stemming ones. The conclusion is that there is a real knife effect. It bends the molecules or cuts them in a manner depending on their orientations. This produces fracture

surfaces that more or less reveal the initial structure. Such a phenomenon cannot exclude further irradiation effects since these are well documented in many other studies such as those reported in the introduction. A comparison of non-irradiated and irradiated surfaces as observed by AFM will demonstrate these changes.

## 6. Modifications due to radiation: comparison of non-irradiated and irradiated surfaces

Figs. 3–5 of the preceding sections show different views of the same specimen. Fig. 5 (AFM) was recorded before the specimen was irradiated in TEM (Fig. 3) and then observed in AFM (Fig. 4). A direct comparison shows that the periodic cholesteric surface has changed under the effect of the irradiation. Whereas the non-irradiated surface looks uneven with many knife tracks and short discontinuous faint periodic lines, the periodicities on the irradiated surface are now very regular and continuous. The knife tracks have disappeared. Other features in the form of small bows aligned parallel along the ridges are also well pronounced in the irradiated specimen. They are already present in a native way in some non-irradiated specimens. These modifications indicate that a part of the surface has been removed and etched, so that hidden internal features appear clearly. To shed further light on this phenomenon, we focused the TEM electron beam as a small intense spot on the specimen, 2 μm in diameter, with an electron density of 5000 e/nm$^2$ s during 15 s. We then enlarged the beam to take the micrograph of the whole irradiated specimen, which was then examined in AFM. Fig. 9 shows an example of a hollow, about 45nm deep, formed by irradiation in this way. This is a strong indication of material being removed.

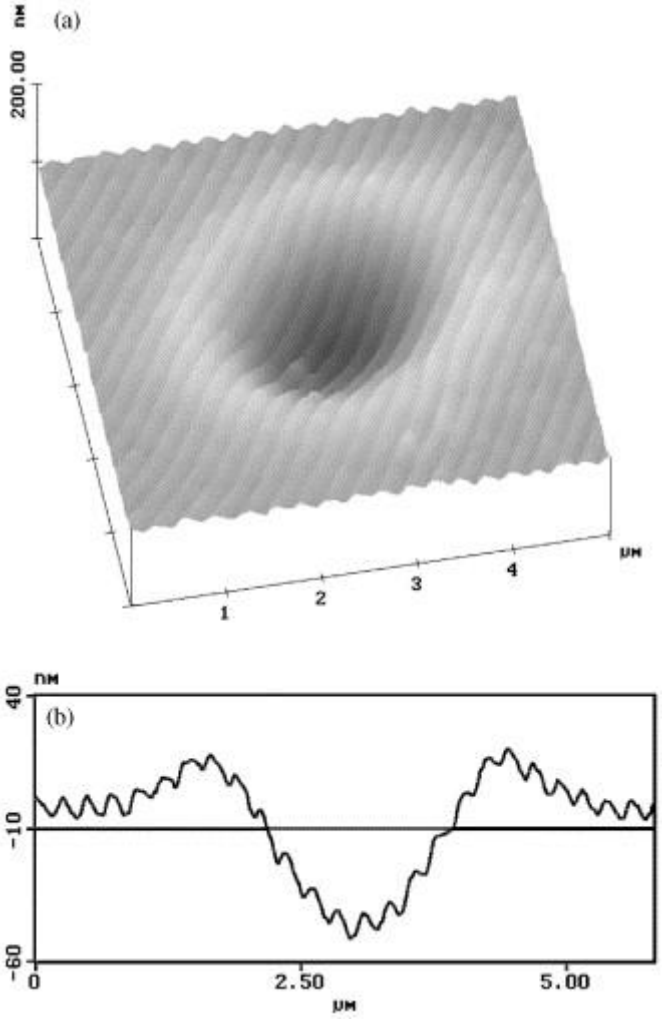


Fig. 9. Hole in a cholesteric structure due to a strongly convergent electron beam. Periodicities are still visible in the bottom. (a) 3D image; (b) profile along a line perpendicular to the periodicities.

At the bottom of the hollow, the corrugations are similar to those of the upper surface, showing that the material has been removed faster but homogeneously. This is not the case at the boundary where a strong slope has formed, surrounded by a circular ruff about 20 nm high. Evaporation or sublimation of material is not surprising since mass loss due to irradiation was reported in polymers including embedding resins [5–8, 26]. For example, Eddie and Karlson [27] measured the decrease of thickness of Formar films. Heavens et al. [28] recorded a similar diminution of thickness in polyoxymethylene occurring in scanning electron microscopy (SEM) in various dose conditions. The mass loss is also perceptible in electron energy-loss spectra

of polymers [29,30]. If mass loss occurs and create corrugations in a cholesteric film, it should also occur in other structures. We checked it by focusing the electron beam in TEM (7 μm in diameter, 5000 e/nm$^2$ s during 15 s) on an embedding resin (Epoxy resin) around the cholesteric structure, then AFM images were taken (Fig. 10).

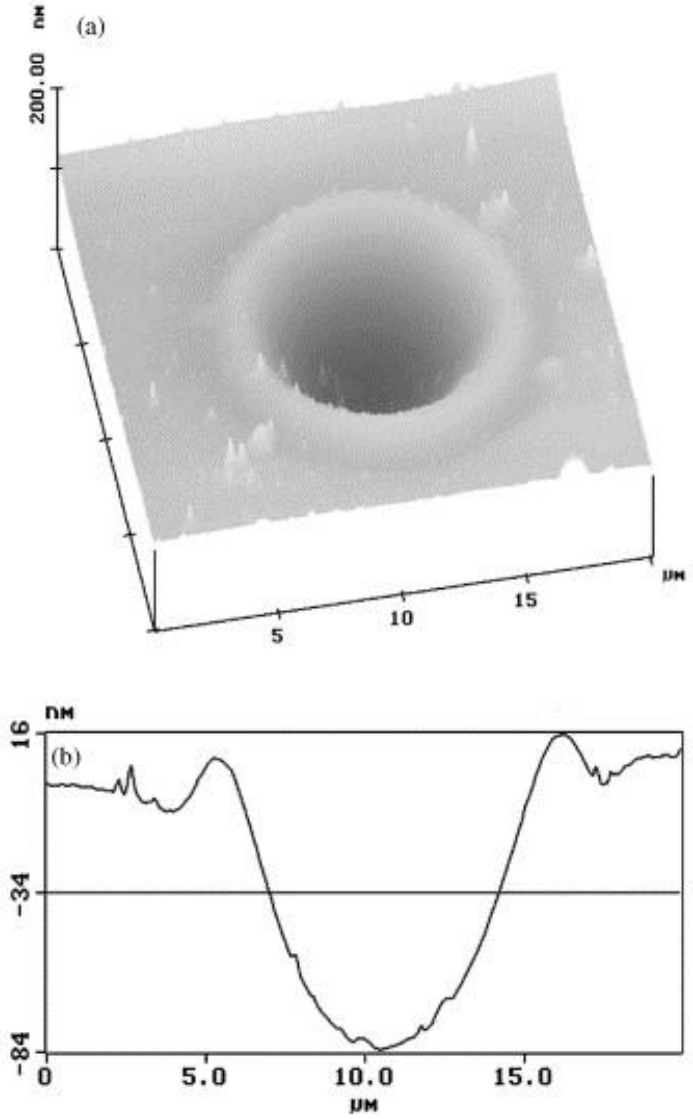


Fig. 10. Hole produced in the same manner as in Fig. 9 in the embedding resin. (a) 3D image; (b) profile along a diameter.

A 94 nm deep hollow has been bored and a 20 nm high ruff around the boundary is also present. Material has been removed in the same way as on the cholesteric film surface. Other

images taken at the boundary between the resin and the cholesteric structure (Fig. 11) show that etching is faster in resin.

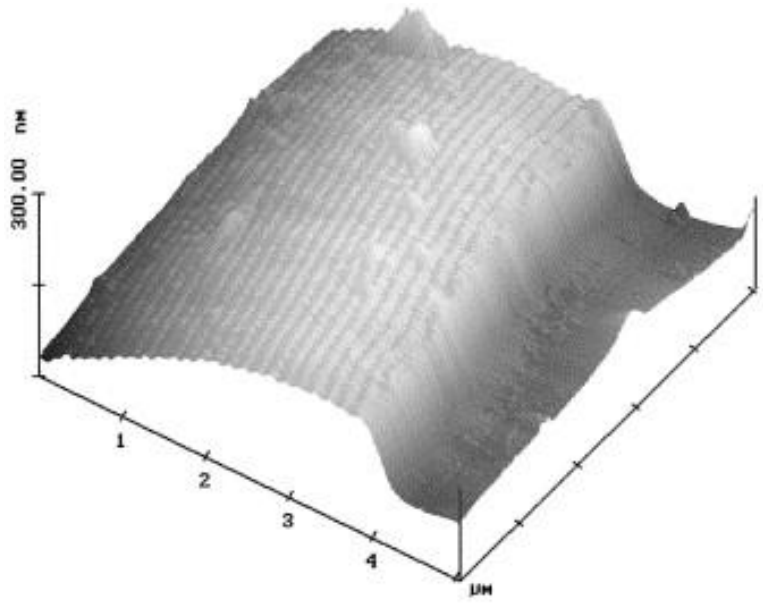


Fig. 11. An area eroded in the same manner at the boundary between the resin and the cholesteric structure. 3D image.

An irradiation test has also been made in a self-supported resin in order to establish what happens at the lower surface. The absence of the carbon substrate allows the resin to be viewed from both faces. On the upper side, the hollow is the same as in the carbon supported resin (Fig. 10). The bottom side shows a bump that has exactly the same profile as the hole. This means that, at least in this case, the resin has sunk as a whole. But this mechanism does not operate in the case of a carbon supported resin, where there is a limited possibility for the film to sink. TEM images show that the area of the spot impact is recognisable by its clearer aspect, which is evidence that the area is thinner. Therefore, the decrease of the thickness is clearly demonstrated.

## 7. Etching and molecular orientation

A possible explanation of the formation of very regular periodic ridges on the surface is that the initial relief made by the knife is enhanced by etching. The valleys become deeper valleys and the ridges remain ridges. However, if we are to conclude that the corrugations become more regular than in non-irradiated specimens, and that they even appear on specimens with no initial ridges after cutting (Fig. 6), it has to be assumed that the irradiation mechanism is also dependent on the initial molecular orientations: the areas are hollowed at different depths according to their orientation. To check this hypothesis and determine which orientation is deeper etched, we recorded a diffraction contrast image, from which the molecular orientation can be determined. A comparison of the contrast before and after radiation damage in the same micrograph was made by exposing to the electron beam only a part of the sample area viewed on the screen. The beam is focused in the central part of the micrograph to produce an irradiation contrast, while the diffraction contrast was preserved in its outer part exposed only during the time of micrograph (Fig. 12). Surprisingly, the dark lines from the irradiated part exactly match the dark lines from the non-irradiated part, although the mechanism of contrast is completely different. A difference is that the bright lines are brighter in the irradiated part than in the non-irradiated part. It is deduced that the molecules in the ridges are horizontal and parallel to the lines.

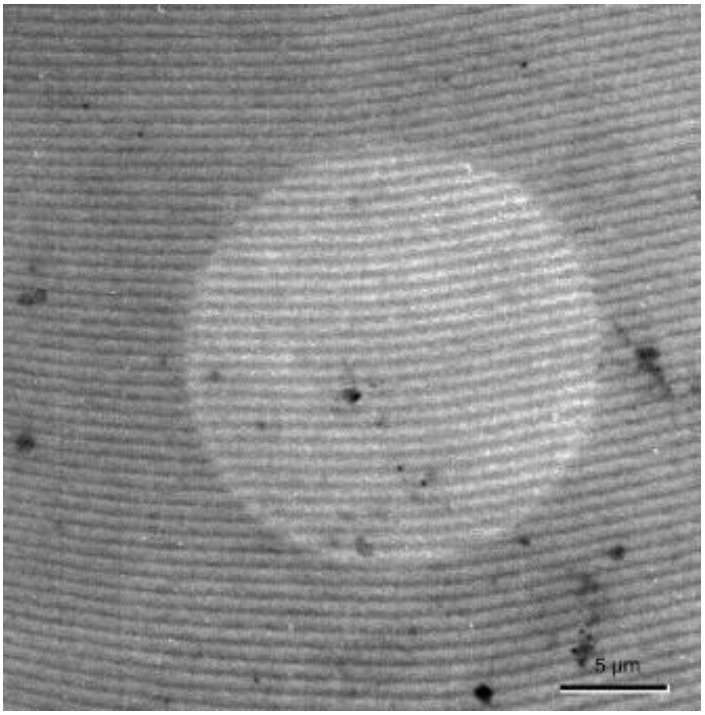


Fig. 12. Section of the cholesteric film observed in TEM (bright field). Irradiation contrast in the light central part, with a lower thickness. The outer part has been preserved from the radiation except during the micrograph exposure, and displays a diffraction contrast. Both contrasts exactly match.

## 8. Discussion and conclusion

The processes leading to a contrast in glassy cholesteric structures observed in TEM are summarized in Fig. 13.

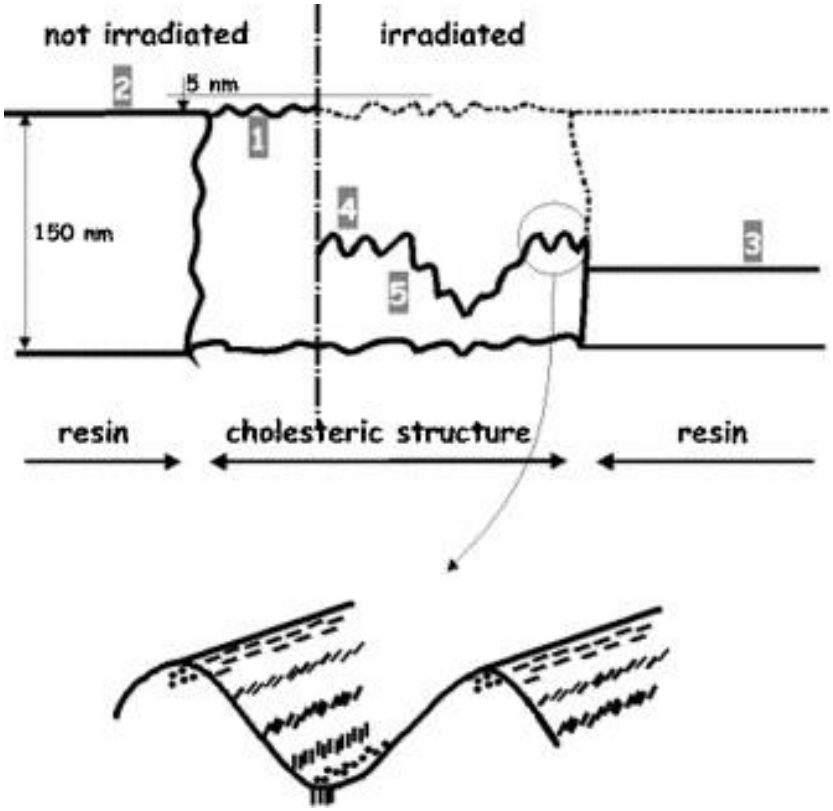


Fig. 13. A sketch summing up the proposed mechanism of the cholesteric contrast in TEM. It combines the effects of the ultramicrotome knife and of the irradiation. Left: before irradiation. Right: after irradiation. (1) Erratic corrugations produced by the knife on the cholesteric structure. (2) Flat cut surface on resin. (3) Mass loss due to irradiation in resin. (4) Mass loss due to irradiation in cholesteric structure enhancing corrugations, the more intense is the beam.
(5) Local deformation inside the specimen.

First, the ultramicrotome knife fractures the specimen along a surface of least resistance. This surface is sometimes random and sometimes reveals the internal cholesteric molecular orientations as described by Bouligand (Figs. 1 and 7 and point 1 in Fig. 13). The fracture surface in the resin is flat and even (point 2 in Fig. 13). As irradiation by the electron beam proceeds, the molecular cholesteric order is lost. This behaviour is thus similar to that of crystalline polymers, which lose their crystalline diffraction pattern because of radiation damage. This means that the anisotropy disappears and gives way to a spherical symmetry that does not give rise to any contrast. In crystalline polymers, this is known to be due to crosslinking and it is likely that the same process is responsible in liquid crystals. At the same

time, scission of macromolecules is responsible for mass loss and decrease of thickness. The rate of decrease is a function of the intensity and time of irradiation as illustrated by Figs. 9 and 10. It also depends on the material studied, since the embedding resin becomes thinner faster than the SB–SR cholesteric material (point 3 in Fig. 13). In the liquid crystal, etching is faster where the molecules are vertical and it produces valleys (point 4 Fig. 13). We now discuss a possible mechanism to account for this process. At the molecular level, the basic processes of irradiation are chain scission and creation of radicals resulting in mass loss, chain cross-linking and local deformation (radiochemistry [31]), and they are responsible for effects at a submicron level, different for different molecular oriented areas. We propose that the link between these two levels consists of several cooperative processes acting together at variable degrees: electron beam channelling, and differential deformation, with differential etching being the more important process, as discussed below. To our knowledge, electron beam channeling has never been taken into account in the process of radiochemistry, though we have demonstrated its existence in polyethylene single crystals [9]. It is known [32] that the beam intensity varies inside an ordered lattice such as a crystalline lattice cell, and that for some orientations of the beam with respect to the lattice plane, the Bloch waves are channelled along the atom columns. We calculated for polyethylene that the intensity could be multiplied by 1.5–3, as a function of the orientation of the specimen and of the depth of the electron wave plane. The effect is more pronounced when the thickness increases but it is offset by the absorption due to inelastic scattering. An optimum was found for polyethylene at a thickness of about 20–100nm, for voltages between 300 and 3000 kV. This effect should be valid in an oriented liquid crystal since the electron waves are channelled in a different way according to the molecule orientation. It may account for the variation of chain scission and etching according to the orientation of the molecules. It is likely that the intensity increases along the vertical molecules more than from one horizontal molecule to another. More chain scissions or more radicals are then produced. They migrate easily along the vertical molecules up to the upper surface while the bottom is protected by the carbon substrate. Mass loss is thus more

effective for the vertical molecules. This effect can be enhanced by a better resistance to irradiation by horizontal molecules due to self-healing (differential etching). Self-healing is the process by which two pieces of molecules resulting from chain scission or two radicals recombine as they were initially [9]. An alternative mechanism to account for the formation of ridges is to assume that the molecules expand laterally. This has already been noticed by Grubb et al. [12] in polyethylene single crystals. The expansion was found to occur perpendicularly to the chain axis. The explanation was a reduction of the end-to-end distance of the chain, which tends to become a statistical coil when crosslinking develops. Applied to the cholesteric structure, this deformation moves vertical molecules laterally in the substrate plane and thus the area becomes thinner. Where they are horizontal, they expand perpendicularly to the substrate and are also pushed by the vertical molecules that have moved, with the result that the area becomes thicker (point 5, Fig. 13). We think however that this phenomenon is restricted in these cholesteric materials by the stiffness of the mesogenic moieties that do not have the same tendency to coil and to shorten as the flexible polyethylene molecules. The existence of a ruff around the beam impact spots could also support the evidence of deformation mechanisms, since the ruff seems to rise up from material pushed from the slope. But the existence of such a ruff also in amorphous epoxy resin indicates that the deformation is not related to variously oriented molecules in this particular transition area. Rather, temperature differences due to the intense beam focusing and electrical differences if the electric charges are not well evacuated create stresses strong enough to disturb this zone.

## Acknowledgements

We thank F.H. Kreuzer (Wacker Chemie Ltd.) for providing us with cholesteric materials, C. Binet for the preparation of liquid crystal specimens, L. Dubac for her help in AFM, and P. Hawkes for correcting our mistakes in English.

## References

[1] L.C. Sawyer, D.T. Grubb, Polymer Microscopy, Chapman and Hall, London, 1994.

[2] H. Ringsdorf, R. W.ustefeld, Philos. Trans. R. Soc. London A 330 (1990) 95.

[3] M. Mitov, A. Boudet, P. Sop!ena, Eur. Phys. J. B. 8 (1999) 327.

[4] A. Boudet, C. Binet, M. Mitov, C. Bourgerette, E. Boucher, Eur. Phys. J. E 3 (2000) 247.

[5] L. Reimer, in: B.M. Siegel, D.R. Beaman (Eds.), Electron Microscopy and Microbeam Analysis, Wiley, New York, 1975, p. 231.

[6] K. Stenn, G.F. Bahr, J. Ultrastruct. Res. 31 (1970) 526.

[7] R.M. Glaeser, in: B.M. Siegel, D.R. Beaman (Eds.), Electron Microscopy and Microbeam Analysis, Wiley, New York, 1975, p. 205.

[8] D.T. Grubb, J. Mater. Sci. 9 (1974) 1715.

[9] A. Boudet, C. Roucau, J. Physique 46 (1985) 1571.

[10] A. Boudet, J. Physique 47 (1986) 1043.

[11] J. Duglosz, A. Keller, J. Appl. Phys. 39 (1968) 5776.

[12] D.T. Grubb, A. Keller, G.W. Groves, J. Mater. Sci. 7 (1972) 131.

[13] T.J. Bunning, D.L. Vezie, P.F. Lloyd, P.D. Haaland, E.L. Thomas, W.W. Adams, Liq. Cryst. 16 (1994) 769.

[14] J. Pierron, A. Boudet, P. Sop!ena, M. Mitov, P. Sixou, Liq. Cryst. 19 (1995) 257.

[15] Y. Huang, Y.Q. Yang, J. Petermann, Polymer 39 (1998) 5301.

[16] A. Hauser, H. Kresse, A. Glushchenko, O. Yaroshchuk, Liq. Cryst. 26 (1999) 1603.

[17] R. Meister, H. Dumoulin, M.A. Hall!e, P. Pieranski, J. Phys II France 6 (1996) 827.

[18] B.D. Terris, R.J. Twieg, C. Nguyen, G. Sigaud, H.T. Nguyen, Europhys. Lett. 19 (1992) 85.

[19] M. Mitov, P. Sixou, Mol. Cryst. Liq. Cryst. 231 (1993) 11.

[20] J. Pierron, V. Tournier-Lasserve, P. Sop!ena, A. Boudet, P. Sixou, M. Mitov, J. Phys II 5 (1995) 1635.

[21] F.H. Kreuzer, D. Andrejewski, W. Haas, N. Haberle, G. Riepl, P. Spes, Mol. Cryst. Liq. Cryst. 199 (1991) 345.

[22] C. Binet, M. Mitov, A. Boudet, Mol. Cryst. Liq. Cryst. 339 (2000) 111.

[23] M.M. Giraud-Guill!e, Tissue and Cell 18 (1986) 603.

[24] Y. Bouligand, Tissue and Cell 18 (1986) 621.

[25] V. Tournier-Lasserve, A. Boudet, P. Sop!ena, Ultramicroscopy 58 (1995) 123.

[26] M.K. Lamvik, J. Microsc. 161 (1991) 171.

[27] J.W. Eddie, U.L. Karlson, J. Microsc. 13 (1972) 13.

[28] J.W. Heavens, A. Keller, J.M. Pope, D.M. Rowell, J. Mater. Sci. 5 (1970) 53.

[29] M. Isaacson, Ultramicroscopy 4 (1979) 193.

[30] R.F. Egerton, I. Rauf, Ultramicroscopy 80 (1999) 247.

[31] G. Ungar, J. Mater. Sci. 16 (1981) 2635.

[32] J.C.H. Spence, J.M. Zuo, Electron Diffraction, Plenum Publishing Corporation, New York, 1992.